Experimental Brain Research (2019) 237:2481–2493
https://doi.org/10.1007/s00221-019-05605-z

RESEARCH ARTICLE

# Intracerebroventricular administration of histidine reduces kainic acid-induced convulsive seizures in mice

**Serdar Alpdogan[1] · Felix Neumaier[1] · Maxine Dibué-Adjei[1,2] · Jürgen Hescheler[1] · Toni Schneider[1]**

Received: 25 April 2018 / Accepted: 13 July 2019 / Published online: 18 July 2019
© Springer-Verlag GmbH Germany, part of Springer Nature 2019

## Abstract

Kainic acid (KA)-induced seizures and other experimental models of epilepsy have been proven to be instrumental in identifying novel targets that could be responsible for human icto- and epileptogenesis. We have previously shown that the ablation of pharmacoresistant voltage-gated $Ca^{2+}$ channels with $Ca_v2.3$ as central ion-conducting pore (R-type $Ca^{2+}$ channel) reduces the sensitivity towards KA-induced epilepsy in mice. In vivo, $Ca_v2.3$ channels are thought to be under tight allosteric control by endogenous loosely bound trace metal cations ($Zn^{2+}$ and $Cu^{2+}$) that suppress channel gating via a high-affinity trace metal-binding site. Metal dyshomeostasis in the brain, which is a common feature of (KA-induced) seizures, could therefore alter the normal function of $Ca_v2.3$ channels and may shift hippocampal and neocortical signaling towards hyperexcitation. To investigate the role of loosely bound metal ions for KA-induced hyperexcitation in vivo, we examined the effects of manipulating brain trace metal homeostasis in mice. To this end, we developed a murine system for intracerebroventricular administration of trace metal ions and/or histidine (His), which can bind $Zn^{2+}$ and $Cu^{2+}$ and is involved in their transendothelial transport at the blood–brain barrier. Unexpectedly, our preliminary findings indicate that application of His alone but not in the presence of $Zn^{2+}$ has substantial beneficial effects on the outcome of KA-induced epilepsy in mice. As such, our results emphasize previous findings on the complex, two-sided role of loosely bound metal ions with regard to neuronal excitation and degeneration under pathophysiological conditions.

**Keywords** Plastic cannulas · Telemetry · Trace metal cations · Pharmacoresistant calcium channel · R-type

## Introduction

Expression and function of voltage-gated $Ca^{2+}$ channels (VGCCs) are under tight cellular control. In mammals, ten members of VGCCs are known: L-($Ca_v1.1$, $Ca_v1.2$, $Ca_v1.3$ and $Ca_v1.4$), P/Q-($Ca_v2.1$), N-($Ca_v2.2$), R-($Ca_v2.3$), and T-type ($Ca_v3.1$, $Ca_v3.2$, and $Ca_v3.3$) (Catterall 2011). Several ion-conducting $Ca_v\alpha_1$ subunits (Lee et al. 1999; Kang et al. 2006) and many native $Ca^{2+}$ currents (Kiss and Osipenko 1994; Büsselberg et al. 1994) are antagonized by inorganic cations, which have long been used to block voltage-gated $Ca^{2+}$ channels [for review, see (Neumaier et al. 2015)]. The pharmacoresistant voltage-gated $Ca^{2+}$ channel (R-type) containing the $Ca_v2.3$ α1 subunit as ion-conducting pore (Perez-Reyes and Schneider 1994) was especially shown to be among the most sensitive molecular targets of $Cu^{2+}$ currently known (Shcheglovitov et al. 2012). Low nanomolar concentrations are sufficient to tonically inhibit these channels and to markedly shift voltage-dependent gating towards more depolarized potentials. Structurally, the exceptionally high sensitivity results from two histidine residues in the IS3–IS4 loop ($His^{179}$ and $His^{183}$) and a third one located in the IS1–IS2 loop ($His^{111}$) of the $Ca_v\alpha1$ subunit (Kang et al. 2007; Shcheglovitov et al. 2012). Thus, the binding site for $Cu^{2+}$ but also for $Zn^{2+}$ is located outside the cell, but the blood–brain barrier inhibits easy access of administered divalent cations to the R-type $Ca^{2+}$ channels in the nervous system.

The direct instillation of drugs into the intracerebroventricular space has long been used in human pharmacotherapy in a number of disease states of the central nervous system (Cook et al. 2009) and is preferred for antibiotics and antineoplastic drugs, because the administration via this route

✉ Toni Schneider
toni.schneider@uni-koeln.de

[1] Institute for Neurophysiology, University of Cologne, Robert-Koch-Str. 39, 50931 Koeln, Germany

[2] Department of Neurosurgery, Medical Faculty, Heinrich-Heine-University, Düsseldorf, Germany

ensures a more homogeneous drug distribution throughout the cerebrospinal fluid (CSF) space (Atkinson 2017). Molecules and ions, administered into the CSF, are freely exchanged into the extracellular fluid of the brain parenchyma. However, the technique of intracerebroventricular (ICV) administration is "under-utilized" in preclinical research on CNS disorders due to the high degree of technical skill needed for the correct ICV guide cannula implantation. However, these technical challenges can be overcome using standardized procedures and attention to details during the surgery protocol and during the postoperative period (Cook et al. 2009).

In addition, several technical issues have to be considered for the chronic implantation of ICV guide cannulas and the injection of trace metal-containing solutions. (1) To avoid trace metal contamination by metal cannulas, the use of metal-free cannulas is recommended and described in detail. (2) Further, the background level of trace metal contamination in physiological solutions strongly depends on the purity of reagents and type of labware used for preparation and storage as well as during the standard handling procedures. (3) Different from other biologically relevant divalent cations, such as $Ca^{2+}$ and $Mg^{2+}$, free concentrations of trace metals in the brain are extremely low and strictly regulated by a variety of metalloproteins (Valko et al. 2005). In a healthy brain, concentrations of $Zn^{2+}$ and $Cu^{2+}$ are estimated to be around 70–150 µM (Mathie et al. 2006), and most of them (> 95%) are protein bound. Local free or loosely bound concentrations of $Zn^{2+}$ and $Cu^{2+}$ have been proposed to reach 30 µM (Frederickson et al. 2005) and 1.7 µM (Mathie et al. 2006), respectively. Thus, during the injection of trace metals into the ventricles, histidine was used as a chelator instead of metalloproteins, and its application to enable $Zn^{2+}$ injection into the CNS led to unexpected results. Although it has been reported that changes in the brain histidine concentrations are mediated by the anticonvulsants phenobarbital and phenytoin (Honda 1984) and that L-histidine could serve as a beneficial adjuvant for antiepileptic drugs (Kaminski et al. 2004; Li et al. 2005) or ameliorate pentylenetetrazole-induced seizures (Wu et al. 2006), its mechanism of action remains unknown. The present report links the beneficial histidine effects to intracerebroventricular zinc application, which is critical during experimentally induced seizures in mice (Rumschik et al. 2009).

## Materials, methods and surgical procedures

### Injection cannulas and injection conditions

For the in vivo research of trace metal cation injections, the Cannula Infusion System (Bilaney Consultants GmbH, Düsseldorf/Germany) is used. The cannula components are made of polyether ether ketone (PEEK, Plastics One Inc., Roanoke, VA, USA), an advanced biomaterial, which is used in medical implants and for optogenetic studies.

### Telemetry system

Telemetry recordings are performed on conscious mice, after more than 7 days of recovery from the implantation procedures. The conditions for the implantation surgery and the technique of telemetric EEG recording for the mice are described in detail after introducing it for the first time (Weiergräber et al. 2005). The system used here consists of a telemetry implant (PhysioTel® transmitter TA10ETA-F20 from Data Science International, DSI, Lexington, USA). It is used with a nominal sampling rate of 1000 Hz with no a priori filter cutoff.

### Radio telemetric electrocorticographic recording of seizures (EcoG analysis)

Animals are allowed to recover 7–10 days from implantation surgery. They are recorded before and after injection of 15 mg/kg KA i.p. EcoGs are obtained at a sampling rate of 1000 Hz without cutoff from freely moving animals in their cages, placed on the telemetry receiver platforms. NeuroScore 2.1.0 (Datascience International, Lexington, USA) is used to calculate six parameters from the raw data, indicative for convulsive seizures: (1) the total number of spike trains, (2) the total spike train duration (min), (3) the average duration (s), (4) longest duration (s), (5) shortest duration (s) and (6) the average number of spikes per train.

An automated seizure detection protocol has been written to quantify ictal activity. The layout is adapted to the visual inspection of original traces and is based on empirical adaptation performed in our former studies (Dibue-Adjei et al. 2017). The protocol recognizes waveforms shorter than 200 ms in length that are between 2.5- and 25-fold the baseline amplitude as spikes. Spikes occurring in intervals between 30 and 1500 ms are recognized as belonging to a spike train which must be at least 300 ms long and contain a minimum of four spikes. No ictal events were detected in the control condition (before KA injection).

### Chemicals

Unless noted otherwise, reagents were obtained from Sigma-Aldrich and used without further purification (Sigma-Aldrich/Merck, Schnelldorf, Germany). Substances were injected in sterile isotonic 0.9% (m/v) sodium chloride solution (KabiPac®, Fresenius Kabi, Bad Homburg, Germany). $ZnCl_2$ was purchased from Sigma as a stock solution (0.1 M $ZnCl_2$, ordering number 03363) and was further diluted in sterile isotonic 0.9% NaCl to a final concentration of 10 µM

for the intracerebroventricular injection. L-Histidine (99.5%) was purchased from Sigma and was used in a concentration of 1 mM. Glutamate-free kainic acid monohydrate (> 99%) was purchased from Milestone Pharmtech (New Brunswick, NJ, USA).

## Animals and housing

Male mice ($n = 29$) with a mixed genetic background (C57Bl/6 and 129SvJ) and at the age between 12 and 20 weeks ($17.4 \pm 0.4$ weeks with a body weight of $31.0 \pm 0.5$ g) are housed at a constant temperature (20–22 °C) in poly-carbonate cages (32 cm × 16.5 cm × 14 cm) under standardized housing conditions with light on from 7 a.m. to 7 p.m. (light intensity at the surface of the animal cages is between 5 and 10 lx), relative humidity of 40–48% and ad libitum access to food and water. After the implantation procedure, animals are individually housed in separate cages and observed frequently to maintain full recovery after surgery. During the recovery period, body weight is measured daily. The animal experimentation described in the text has been approved by the institutional committee on animal care and has been conducted in accordance with accepted standards of humane animal care. All animal experiments are in line with the European Communities Council Directive 2010/63/EU for the care and use of laboratory animals, and as described in the UFAW handbook on the care and management of laboratory animals.

## Transmitter implantation and placement of the guidance cannulas

### Anesthesia and pain treatment

Mice are anesthetized with 100 mg/kg body weight (BW) ketamine hydrochloride (Ketanest, Parke-Davis/Pfizer, Berlin, Germany) and 10 mg/kg BW xylazine hydrochloride (Rompun® 2% Bayer Vital, Leverkusen, Germany) for transmitter implantation and fixation of guidance cannula. During the whole surgical procedure, mice are placed on a thermoregulated operation table to prevent hypothermia. Carprofen (5 mg/kg) was administered subcutaneously for pain management.

### Surgery procedure for transmitter implantation, and placement of electrodes and cannulas

The time needed for the combined surgery procedure is between 30 and 45 min. The surgery for the implantations was performed on a warming plate (295 mm × 245 mm × 70 mm, MEDAX GmbH & Co.KG, Neumünster, Germany) to keep the body temperature at 37–38 °C (98.6–100.4 °F). To avoid corneal desiccation, eyes are covered with dexpanthenol (Bepanthen®, Hoffmann-La Roche AG) during the implantation period and early recovery. A standard stereotaxic frame, which had been modified to fit the mouse skull anatomy, is used as described previously (Weiergräber et al. 2005). Teeth holder and nose clamp as well as the ear bars have been adapted. After the recovery from the surgery procedure (at least 7 days), the mouse cage is placed on individual receiver plates for the recording of EEGs (Weiergräber et al. 2005).

### Injections

All animals are allowed to recover from the implantation procedure for 7 days before intracerebroventricular injections of histidine or trace metal cations and saline or kainic acid occurred. Baseline EEGs of the mice are recorded 24 h before the injections are started.

ICV injections of trace metal cations are performed under isoflurane gas anesthesia via the implanted guide cannula leading to one of the lateral ventricles, while kainic acid or saline has been injected intraperitoneally. For intraperitoneal injection of saline or kainic acid with a dose of 15 mg/kg, volumes were calculated and related to body weight to 0.1 ml per 10 g body weight.

Both injections were applied simultaneously while the mouse was under isoflurane anesthetic. Immediately after both injections were completed, the mice were transferred from their cages with breathable air to the receiver plates where the recording was started.

### Injection procedure in detail for trace metal cations

(1) After recording spontaneous EEGs as a baseline control, the mouse is anesthetized with isoflurane while applying $ZnCl_2$ (10 µM $ZnCl_2$ + 1 mM histidine in saline) or histidine only in saline via the guide cannula. The injection speed was 1.5 µl per min and in total 3 µl.
(2) Injection of kainic acid (15 mg/kg body weight in saline) or saline intraperitoneally 0.1 ml/10 g body weight.
(3) The mouse is placed back into its cage and the receiver plate and recordings and behavioral observations are started.

**Verification of the cannula position and access to the brain ventricle** Postmortem Indian ink is injected through the guide cannula with an injection cannula. The brain is fixed in 4% paraformaldehyde and extracted from the skull. The brain is cut in half in the sagittal plane and the spread ink is found in all four ventricles (Fig. 1), assuming that the guide cannula has been properly placed over the lateral ventricle.

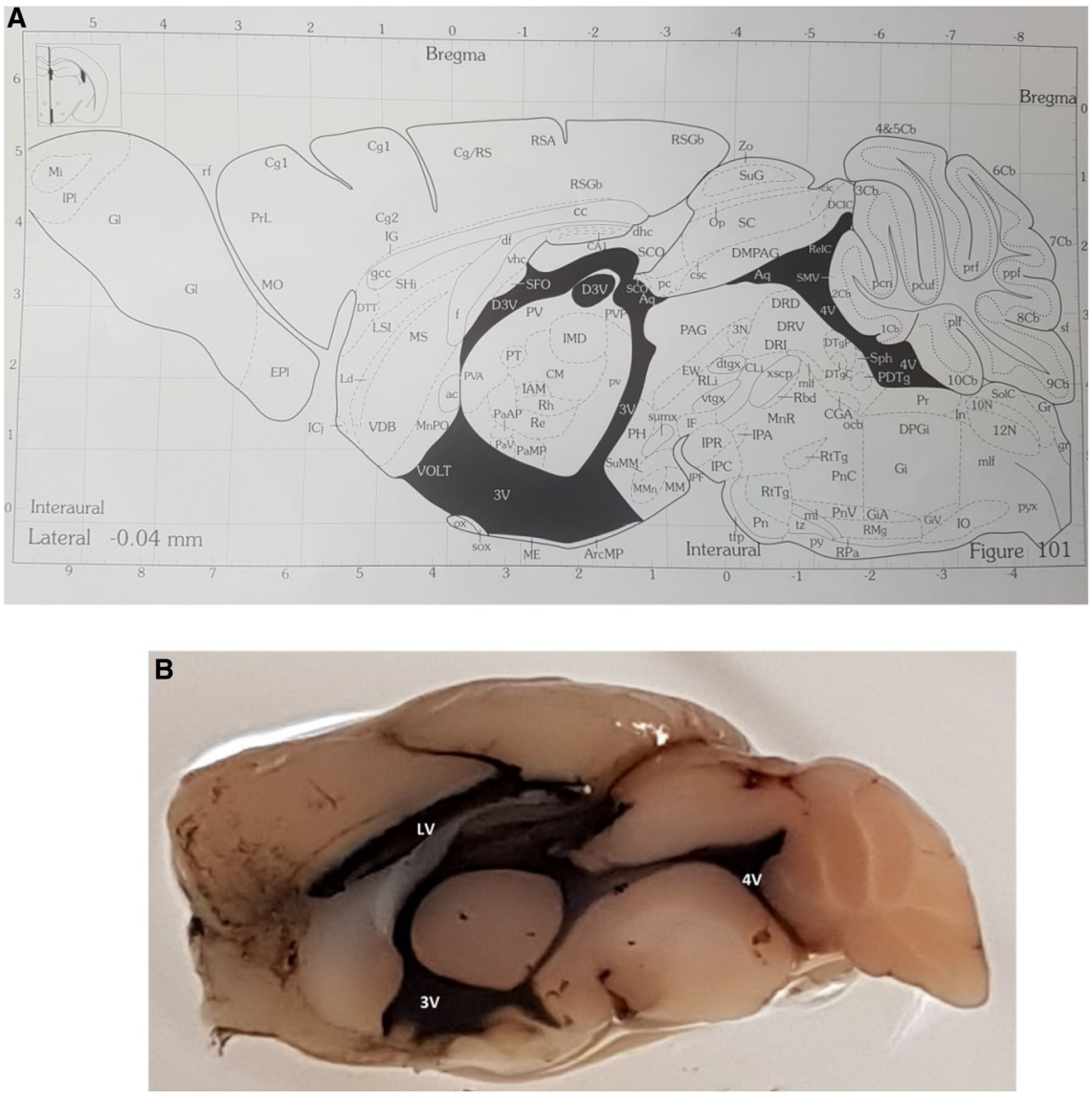


**Fig. 1** Verification of ventricle access by injecting Indian ink postmortem. **a** Side view of murine ventricle from the Paxinos atlas. **b** Side view of a postmortem brain after injection of Indian ink through the injection cannula from the experiment

### Data analysis and statistics

All values are expressed as mean ± SEM based on *n*, the number of independent experiments. Statistical significance was assessed with the unpaired Student's *t* test. *P* values of 0.05 and below were considered significant.

## Results

### Postoperative recovery and cannula implantation

Mice were monitored daily after surgery to check for infection, pain or discomfort and treated when necessary with analgesics (5 mg/kg twice a day carprofen). Pain and discomfort were recognized in individuals by analyzing behavioral changes such as lowered locomotion, lowered grooming behavior, lowered food intake and also by evaluating the appearance of the mouse, for example, if the area around the eyes has narrowed or the cheek and nose has bulged. Moistened and softened food pellets were given to facilitate food and liquid intake during the first 2 days. Eating normal pellets and normal nesting behavior as well as fur care and explorative behavior was observed at the latest after 2–3 days after the surgery. Body weight was followed up and used as an additional measure for progress during recreation (Table 1). Subcutaneous implantations and intracerebral lead placements in mice, as performed

**Table 1** Postoperative recovery of body weight after implantation of radiofrequency transmitter and cannula

| Days after implantation | 0 | 1 | 2 | 3 | 4 | 5 | 6 | 7 |
|---|---|---|---|---|---|---|---|---|
| Mean (%) | 100 | 98.6 | 99.0 | 98.6 | 101.0 | 100.8 | 99.4 | 99.3 |
| St. dev | n.d. | 4.1 | 5.4 | 4.9 | 5.0 | 2.4 | 4.4 | 4.6 |
| *N* | 46 | 46 | 31 | 20 | 22 | 25 | 34 | 41 |

Development of the net body weight is shown for the days after implantation and was normalized to the initial body weight before the implantation (=100%). The weight of the implanted transmitter 3.9 g was subtracted for each animal. The mean age of the male mice was 17.6 ± 1.6 weeks, and the body weight before surgery was 31.3 ± 2.8 g ($n$ = 46 mice). *St. dev* standard deviation, *SEM* standard error of the mean. The number *N* reflects the number of mice, which were investigated during working days (reduced numbers at day 2–6). Therefore, statistical comparison was performed for the day 7 only. Five mice did not survive the implantation procedure. Three of them had a strong body weight reduction shortly before death to 92.1% (day 3), 89.8 (day 4), 91.4% (day 4). Two of them stayed close to or increased their initial weight (102.8% at day 3 and 105.1% at day 3). The body weight after 7 days of the 41 surviving mice is not significant different from the weight before implantation (Student's *t* test)

in this study are routine in our laboratory and it was found that subcutaneous transmitter placement is associated with less body weight reduction during the first 3 post-surgical days than intraperitoneal implantations (Weiergräber et al. 2005).

During a 2-h pre-injection period before kainate (KA) injection, EcoG traces were analyzed for the total number of spike trains, total spike train duration, average spike train duration, longest and shortest spike train duration, and for the average number of spikes per train (Table 2). The epidural placement of cannulas on the mouse skull did not significantly increase any of these six mentioned parameters, leading to the conclusion that the procedure performed in parallel with the electrode implantation for the ECoG recording does not induce ictal activity by itself before KA was injected.

## EEG recordings after subcutaneous implantation of the transmitter and epidural positioning of the cannulas

In all three groups (Table 3), sensitive EEG traces can be recorded after implantation and postoperative recovery. Individual traces from a mouse out of each group show that during the 2 h priming period, no convulsive seizures were detected (a–c in Figs. 2, 3, 4, 5, 6). During this time period, spontaneous EEG traces were collected lacking any extended spike trains. Epileptic discharges were induced by intraperitoneal injection of KA (15 mg/kg) (d, e in Figs. 2, 4, 6).

As in earlier studies, KA-induced ictal activity started with single spiking (not shown here) and led to an increased frequency of spikes and spike-and-waves (Figs. 2d, e, 4d, e, 6d, e). When seizure activity increased to a generalized

**Table 2** Detection of ictal events by the NeuroScore detection system without or with cannula implantation

| Cannulas implanted, no or yes | Total # of spike trains | Total spike train duration (min) | Average spike train duration (s) | Longest spike train duration (s) | Shortest spike train duration (s) | Average # of spikes per train |
|---|---|---|---|---|---|---|
| No | | | | | | |
| Mean | 7.58 | 0.26 | 0.17 | 0.62 | 0.04 | 0.54 |
| SEM | 3.77 | 0.13 | 0.02 | 0.12 | 0.01 | 0.08 |
| *N* | 13 | 13 | 13 | 13 | 13 | 13 |
| Yes | | | | | | |
| Mean | 8.76 | 0.30 | 0.17 | 0.96 | 0.04 | 0.61 |
| SEM | 3.59 | 0.13 | 0.02 | 0.30 | 0.004 | 0.09 |
| *N* | 33 | 33 | 33 | 33 | 33 | 33 |

As described in the method section, the ECoG traces were analyzed by the DSI software NeuroScore using an adapted protocol. A spike train detector helps to identify repeating spike activity using amplitude-based criteria. An automated seizure detection protocol quantified ictal activity. The protocol recognizes waveforms shorter than 200 ms in length that are between 2.5- and 25-fold the baseline amplitude as spikes. Spikes occurring in intervals between 30 and 1500 ms are recognized as belonging to a spike train which must be at least 300 ms long and contain a minimum of four spikes. All six parameters analyzed are far below the values seen after KA injection (Fig. 7) and none of them is significantly different between the two conditions, without or with implanted cannulas

**Table 3** Injection conditions and number of mice: kainate was injected intraperitoneally (15 mg/kg)

| Groups | Group A | | Group B | | Group C | |
|---|---|---|---|---|---|---|
| Genotype, injected solution | A1. Control group | A2. KA group | B1. Histidine group | B2. Histidine + KA | C1. Histidine + $ZnCl_2$ | C2. Histidine + $ZnCl_2$ + KA |
| Cannula implantation | – | – | + | + | + | + |
| Histidine, ICV, 1 mM | – | – | + | + | + | + |
| $ZnCl_2$ ICV, 10 µM | – | – | – | – | + | + |
| Kainate, IP, 15 mg/kg | – | + | – | + | – | + |
| Isotonic NaCl, IP | + | – | + | – | + | – |
| Number of mice | 6 | 7 | 8 | 8 | 8 | 8 |

Histidine (1 mM) was injected intracerebroventricularly, without or in combination with $ZnCl_2$ (nominally 10 µM)

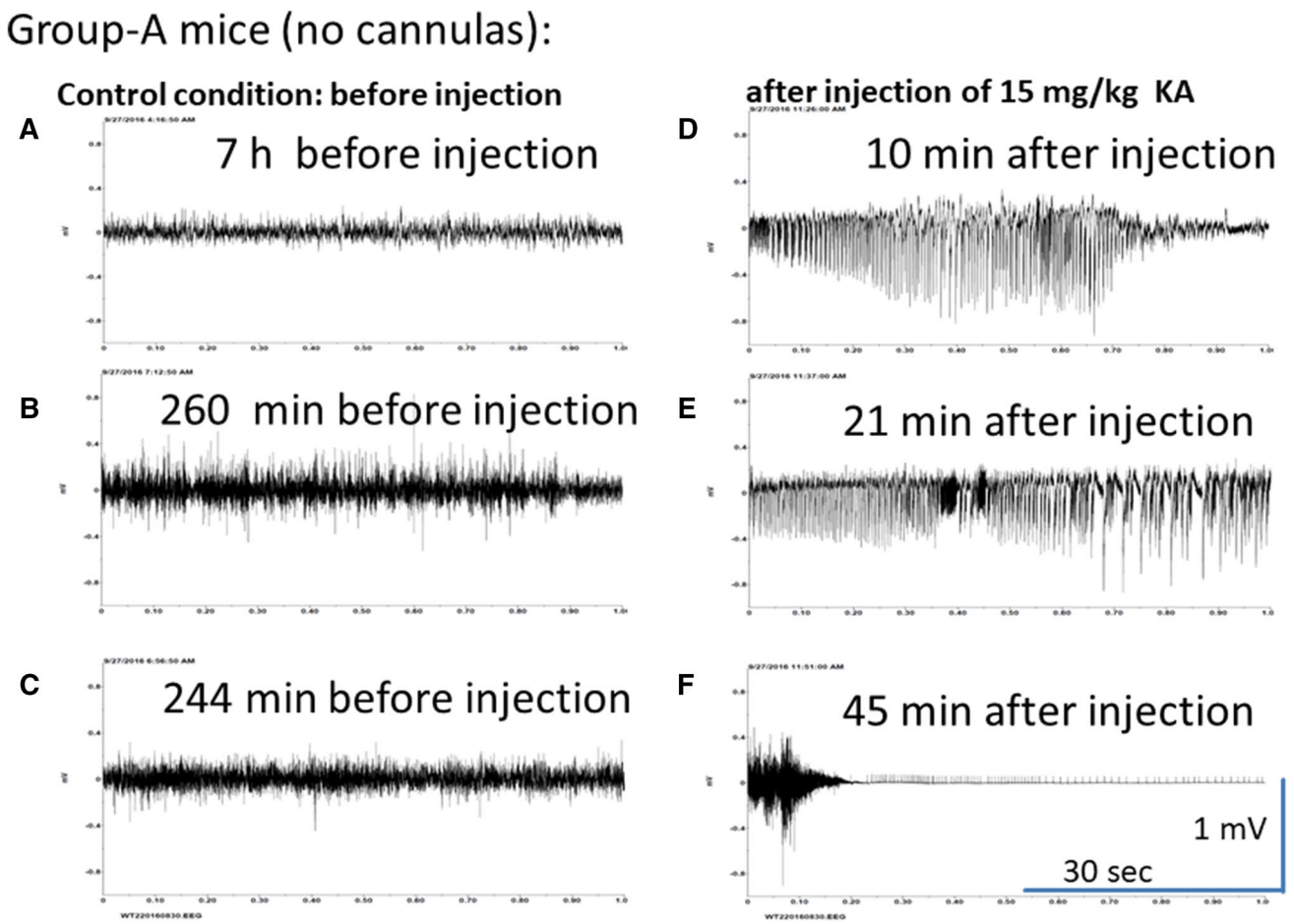


**Fig. 2** Pharmacological induction of epileptic discharges. In Figs. 2, 3, 4, 5 and 6, the PhysioTel® transmitter TA10ETA-F20 was used as the telemetry implant with a nominal sampling rate of 1000 Hz. The software was set to acquire data at 1000 Hz. Raw electrocorticographic traces from an individual control mouse without cannulas (group A2, see Table 3). The recording time before and after KA injection is indicated. **a**–**c** Control traces before KA injection during the routine 2 h observation period. **d**–**f** Development of ictal activity in ECoG after intraperitoneal injection of 15 mg/kg KA. Note that the mouse died during the development of intense ictal activities. The conditions for the implantation surgery and the technique of telemetric EEG recording are described in detail for mice after introducing it for the first time (Weiergräber et al. 2005). The system used here consists of a telemetry implant (PhysioTel® transmitter TA10ETA-F20 from Data Science International, DSI, Lexington, USA) It is used with a nominal sampling rate of 1000 Hz

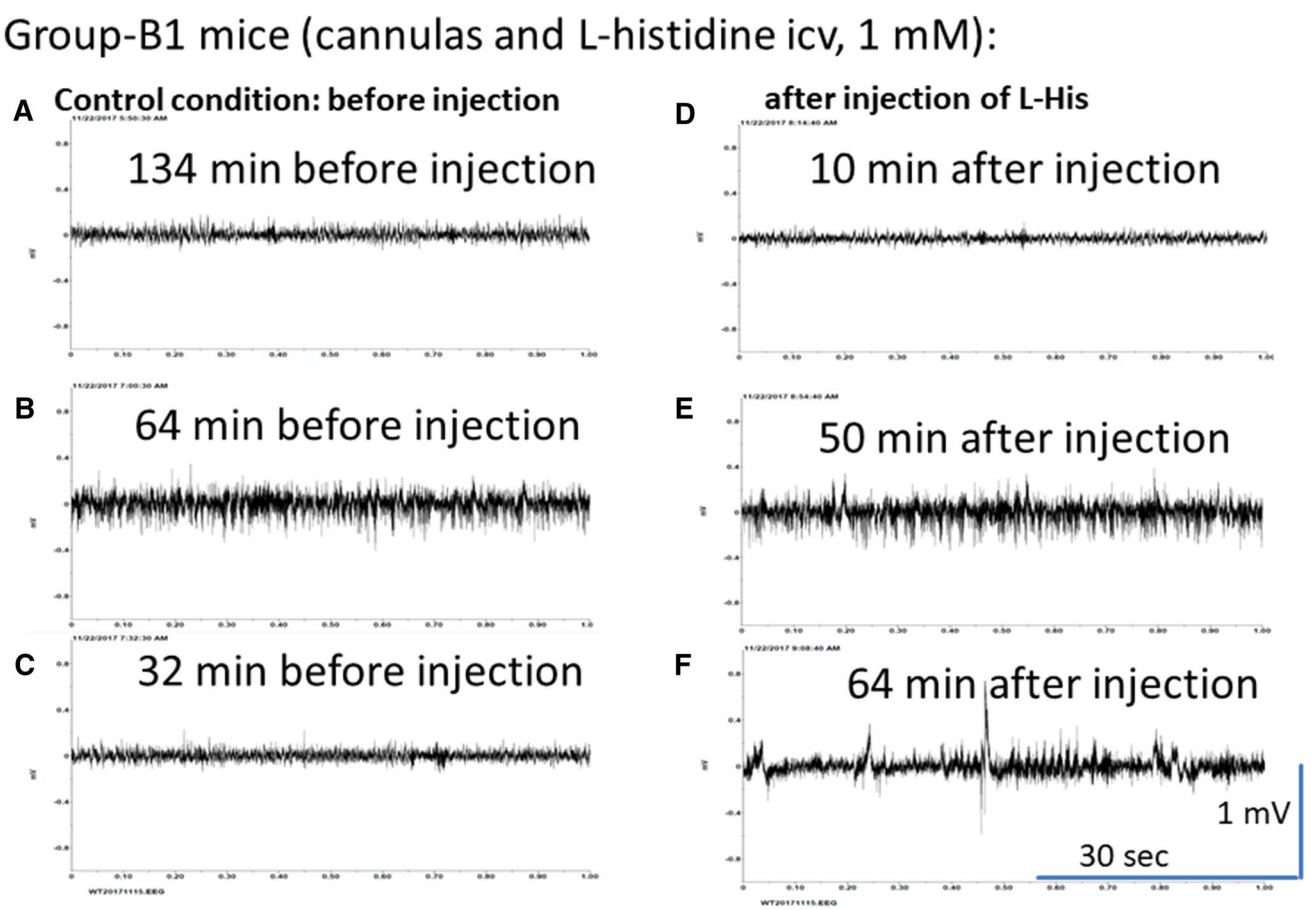


**Fig. 3** Pharmacological induction of epileptic discharges. Raw electrocorticographic traces from an individual mouse in the histidine-injected group B1. The recording time before and after KA injection is indicated. **a**–**c** Control traces before KA injection during the routine 2 h observation period. **d**–**f** Development of ictal activity in ECoG after intracerebroventricular injection of 1 mM L-His

tonic–clonic event, prominent trains of spikes and spike-and-waves arose (Fig. 2), which caused death in five out of eight animals by complications during status epilepticus (Fig. 2f). No epileptic discharges were observed during carrier injections (Figs. 3d, e, 5d, e).

The in-depth investigation of seizure development and characteristics was performed using the NeuroScore software. In group A and C, but not in group B (two data bars in the middle of Fig. 7a–f), the injection of KA (15 mg/kg) significantly increased all the six parameters analyzed by the NeuroScore tool, which confirms the initial observation of a beneficial effect of ICV-injected histidine in group B.

The NeuroScore data are compared in between the three groups. No significant differences in the six parameters were observed for the three conditions without KA injection. But five out of six parameters differ significantly, when group B is compared to group A (see the red bars in Fig. 7a, c–f). Thus, by injecting ICV histidine, the total number of spike trains decreases from $192 \pm 54$ in group A to $43 \pm 26$ in group B (Fig. 7a). The average spike train duration decreased, the longest and the shortest spike train duration as well as the average number of spikes per train also decreased significantly with $P$ values between 0.023 and 0.049 (Fig. 7c–f). Comparing group A data with group C showed a significant difference for the longest spike train duration (see Fig. 7d), which decreased from $84 \pm 30$ s in group A to $20 \pm 4$ s in group C ($P = 0.039$).

When histidine (group B) was injected alone, the total number of spike trains after KA was substantially lower ($43 \pm 26$) than the increase seen in group C ($154 \pm 60$) but did not reach the level of significance (Fig. 7a). Both the total spike train duration ($11.5 \pm 3.3$ [under KA] and $7.2 \pm 2.9$ [under KA + Zn]) (Fig. 7b) and the average spike train duration ($11.4 \pm 4.5$ s vs. $3.9 \pm 0.5$ s) (Fig. 7c) rose to similar values, but they did not reach the level of significance either. However, the longest spike train duration was significantly shorter, either when histidine alone was coapplied with KA ($P = 0.033$) or when $ZnCl_2$/histidine was coapplied with KA ($P = 0.039$) (Fig. 7d). Although the shortest spike train duration, and the average number of spikes per train showed some tendency to be shorter under $ZnCl_2$, it did not reach the level of significance. Obviously, the ictal activity

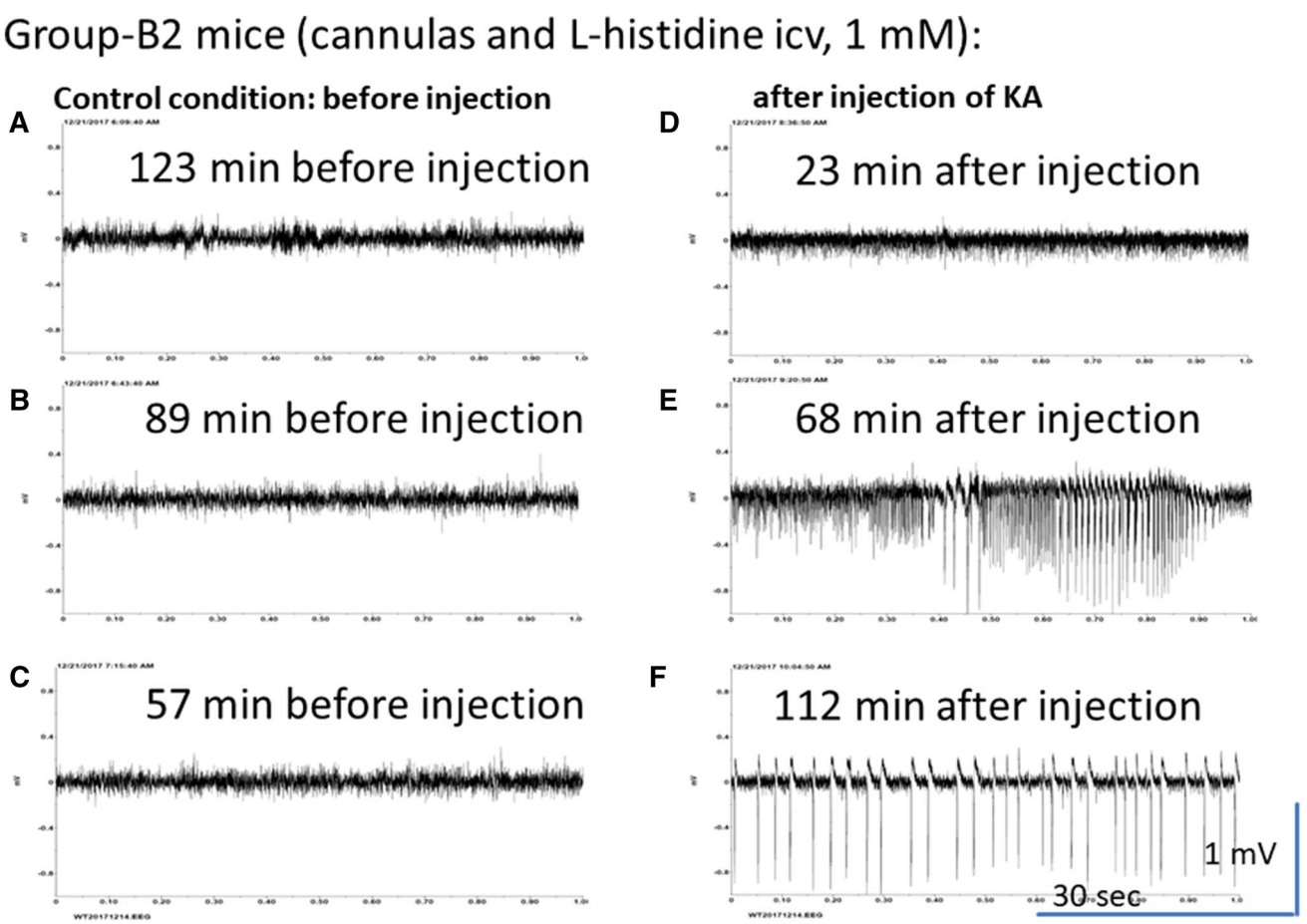


**Fig. 4** Pharmacological induction of epileptic discharges. Raw electrocorticographic traces from an individual mouse in the histidine-injected group B2. The recording time before and after KA injection is indicated. **a**–**c** Control traces before KA injection during the routine 2 h observation period. **d**–**f** Development of ictal activity in ECoG after intracerebroventricular injection of 1 mM L-His and intraperitoneal injection of 15 mg/kg KA

gets milder to a different extent when histidine with or without $ZnCl_2$ is coinjected intracerebroventricularly (Fig. 7).

## Discussion

Using subepidurally implanted cannula co-administered histidine (1 mM i.c.v.) compared to controls was beneficial during kainic acid-induced epilepsy, and adding $ZnCl_2$ together with histidine worsened the outcome after experimentally induced epilepsy. It is unknown how $Zn^{2+}$ prevented the beneficial effects of histidine, but several possible mechanisms will be discussed below. In future, individual mouse lines that lack high-affinity zinc-binding sites will be investigated.

### Precautions during experimentation with low concentrations of divalent bioavailable cations

To administer (divalent) metal cations to the central nervous system successfully, special attention has to be paid to the limited permeability of the blood–brain barrier (BBB) to charged substances. Although the local membrane potential affects the permeability of charged ions through the BBB (Fong 2015), the final flow of ions may be extremely limited so that a cannula injection is advantageous for proper experimentation and drug or ion administration. To avoid any contamination by trace amounts of metal ions from inserted cannula, we deliberately selected plastic cannulas, which were carefully inserted and stably fixed.

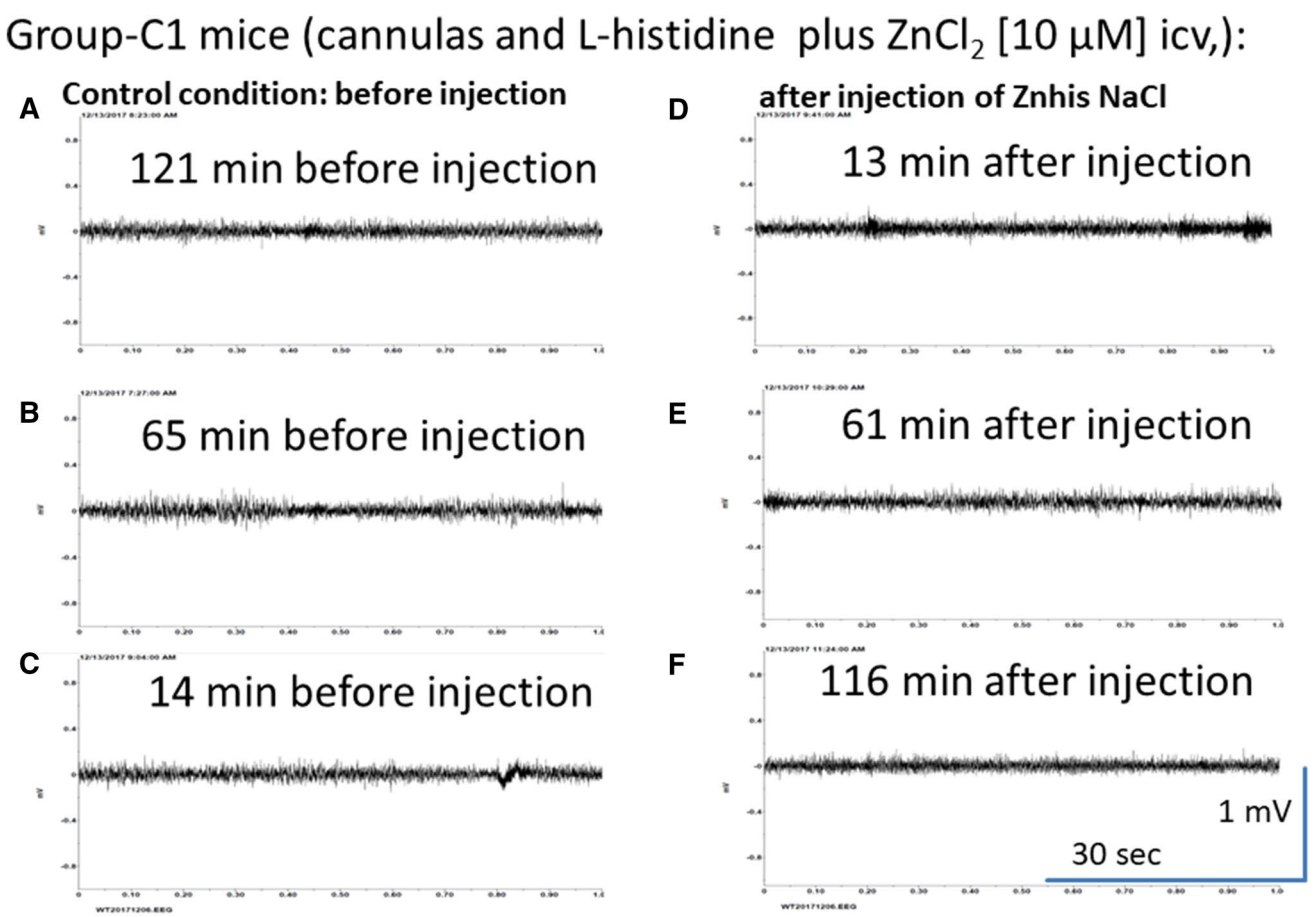


**Fig. 5** Pharmacological induction of epileptic discharges. Raw electrocorticographic traces from an individual mouse in the zinc/histidine group C1. The recording time before and after KA injection is indicated. **a**–**c** Control traces before KA injection during the routine 2 h observation period. **d**–**f** Development of ictal activity in ECoG after intracerebroventricular injection of 10 µM zinc and 1 mM L-His

## Precautions for the interpretation of the post-KA mortality

The interpretation of the NeuroScore data, which were recorded immediately after injection of KA, is hampered by the fact that the mortality differed in the three KA groups. In group A, five out of eight, in group B none out of eight, and in group C four out of eight mice died before the end of the 2 h observation period. The full 2 h period was analyzed by the NeuroScore software, when possible, yielding the parameters in Fig. 7. Four out of the five mice in group A, which died, lived only for 20–40 min, and two out of the four mice dying in group C lived for 50 min. It may be concluded that the severity of convulsive seizures in group A must have been strongest, even stronger than in group C.

Another concern is related to the short duration of time (up to 2 h) for EEG analysis after KA injection. We are confident that during the 2-h observation period, maximal activity changes in the EEG patterns were initialized and that we did not miss them after histidine injection, although we cannot fully exclude this possibility.

## Histidine's anticonvulsant effects

Most surprising was the observation that the beneficial effect of histidine on kainate-induced epilepsy was obscured by adding $ZnCl_2$ (nominally 10 µM). Several explanations have to be considered.

Historically, elevated levels of blood and urinary histidine were found in patients lacking the enzyme histidinase for the normal metabolic breakdown (Arakawa 1974). Some but not all of these patients were even experienced with convulsions and the histidine content was found to be elevated in two cases (Wadman et al. 1966). The spectrum of clinical manifestations of histidinemia was wider in some of these patients and varied from complete normality to gross mental retardation with or without speech defects (Arakawa 1974).

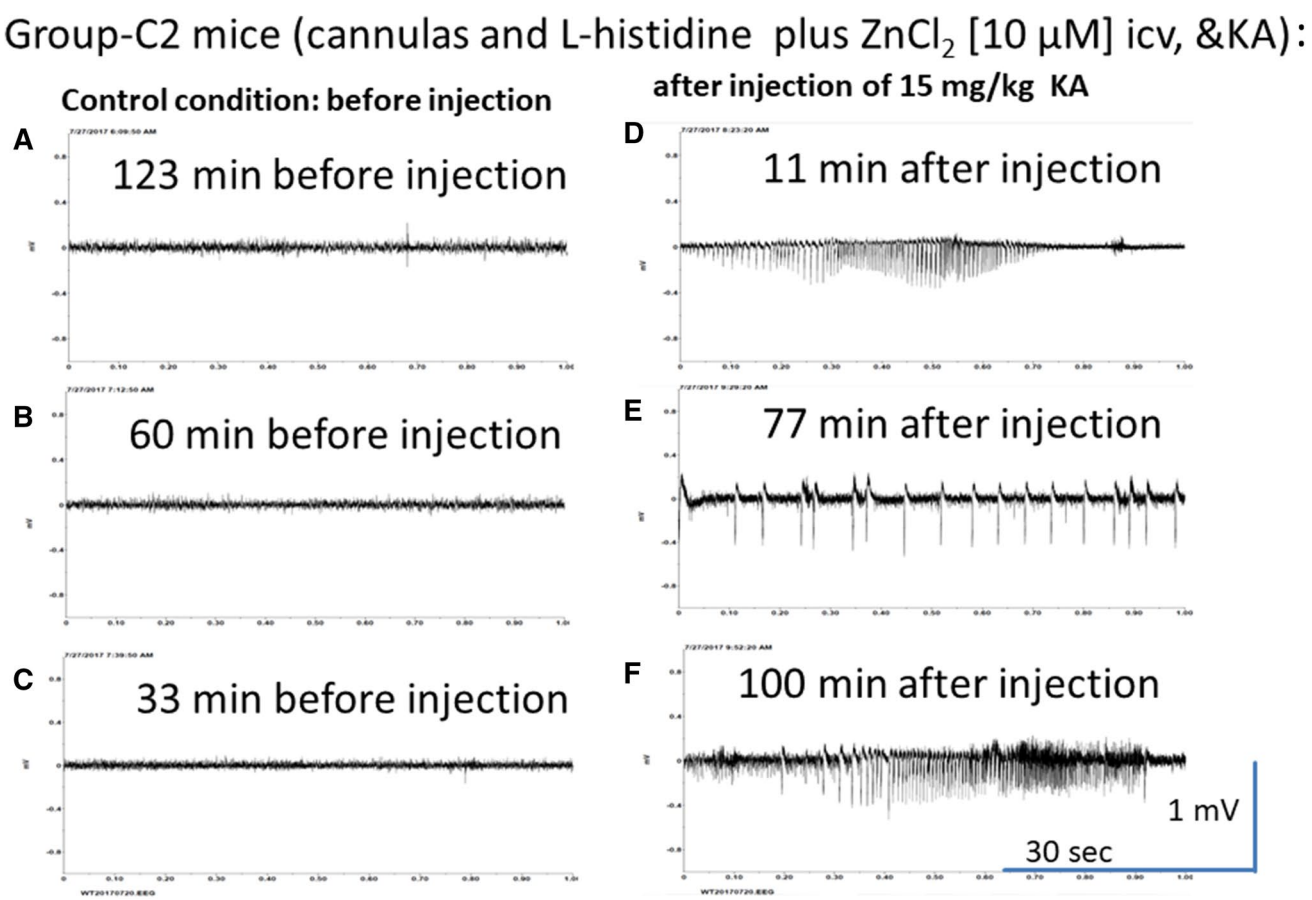


**Fig. 6** Pharmacological induction of epileptic discharges. Raw electrocorticographic traces from an individual mouse in the zinc/histidine group C2. The recording time before and after KA injection is indicated. **a**–**c** Control traces before KA injection during the routine 2 h observation period. **d**–**f** Development of ictal activity in ECoG after intracerebroventricular injection of 10 µM zinc and 1 mM L-His and intraperitoneal injection of 15 mg/kg KA

In 1984, the first hints were found for the amino acid histidine to be important and to be rather beneficial during the treatment of epileptic seizures. The investigation of the free amino acid levels in brains of mice with a convulsive disposition revealed that histidine was increased specifically during administration of the anticonvulsants phenobarbital (120 mg/kg) and phenytoin (60 mg/kg). Some other amino acids also increased under both conditions (glutamine and ornithine). The histidine concentration was unchanged during the administration of control substances like ACTH (0.05 mg) or vitamin B6 (200 mg/kg), but not the concentration of the other mentioned amino acids, which may point to an important role of histidine during modulation of epileptic seizures. Indeed, the beneficial role of histidine, co-administered with antiepileptic drugs, was shown in the following years during electroshock-induced seizures in mice (Kaminski et al. 2004), during chronic transauricular kindling in rats (Li et al. 2005) or during pentylenetetrazole-induced seizures in rats (Wu et al. 2006).

**Fig. 7** Analysis of ECoG traces by NeuroScore. The analysis platform (from DSI) was used to detect seizure events and to quantify them as listed in the table. Using amplitude-based criteria, the seizure detector scans the waveform for repeating spike activity (for details see Dibué-Adjei et al. 2017). The total number of spikes (**a**) and five additional parameters (**b**–**f**) are summarized over a 2 h period. Data from three different groups of mice ($n = 6$–8 animals/group) are compared. Group A mice did not receive any injections and no cannulas were implanted. Group B and group C mice were injected through implanted cannulas either with 1 mM L-histidine only (= group B) or with 1 mM L-histidine plus 10 µM $ZnCl_2$ (group C). Using the Student's *t* test, within each group, statistical significance was tested for the parameters without (no KA) and with kainate injected (+KA). Statistical significance was $P < 0.05$ (*), or $P < 0.01$ (**), or $P < 0.001$ (***)

Our intention to apply histidine during zinc administration was to use it as a carrier system to inject it icv and to help $Zn^{2+}$ to cross the blood–brain barrier. The important role of $Zn^{2+}$ as a neuromodulator in the central nervous

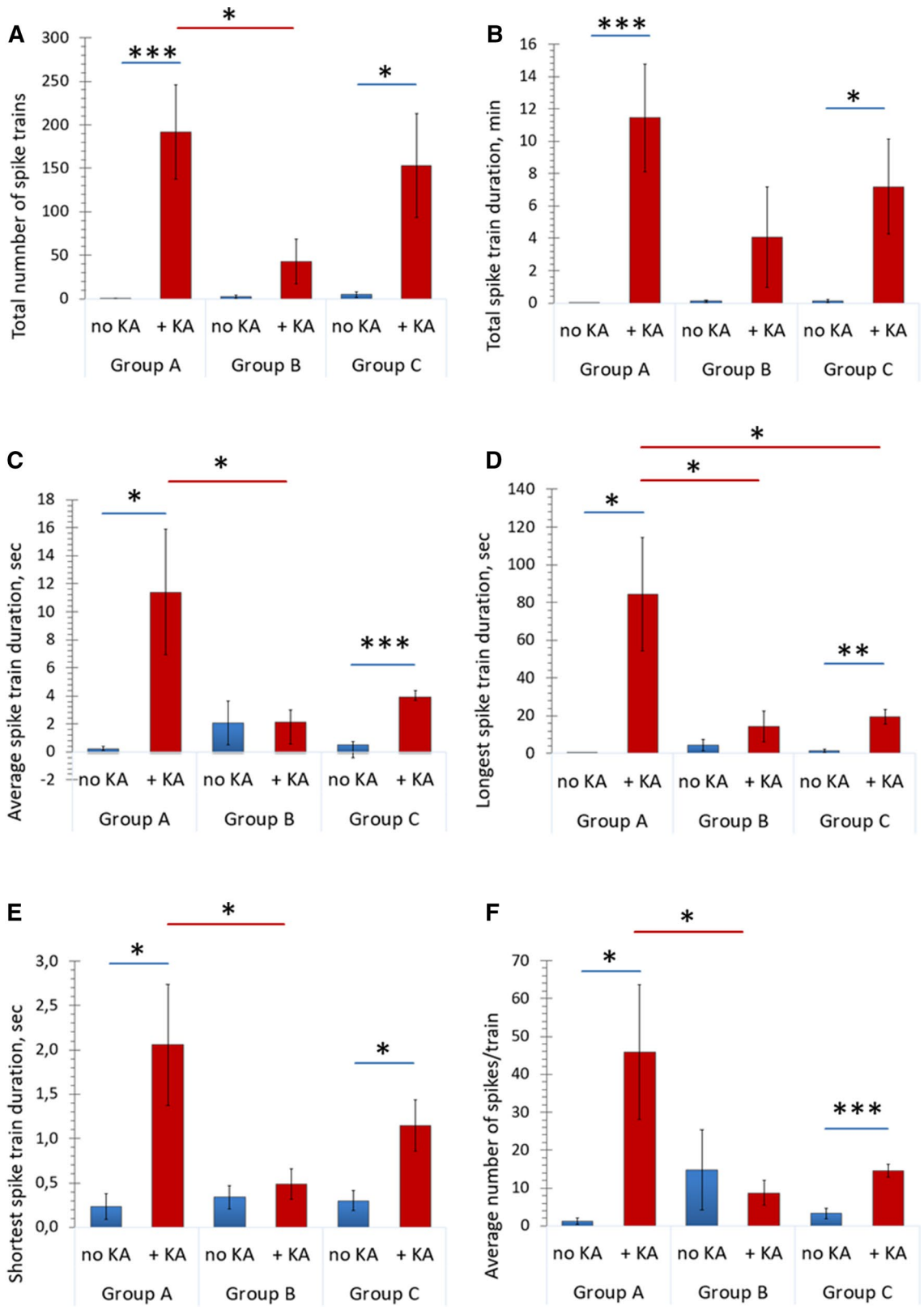


system is widely known (Blakemore and Trombley 2017). It is a common trace element and enriched in multiple brain regions including the hippocampus, the cerebral neocortex and other regions. Even a histidine infusion into the blood vessels enhances the uptake of radiolabeled $Zn^{2+}$ in the brain parenchyma via the CSF (Takeda et al. 2000). Most vesicular

zinc is co-localized with glutamate in a subset of glutamatergic zinc-enriched neurons, but zinc is also contained in the synaptic vesicles of subpopulations of glycinergic and GABAergic neurons [for a recent summary see (Blakemore and Trombley 2017)].

The conversion of histidine to histamine by histidine decarboxylase has been known nearly since 1936 and was discussed intensely during the subsequent years (Edholm 1942). Nearly a dozen of different cell types in the human organism are able to convert this amino acid into histamine, a critical mediator of anaphylaxis, a neurotransmitter and a regulator of gastric acid secretion (Huang et al. 2018). Antagonists of the histamine $H_1$ receptor occasionally induce convulsions in epileptic patients, healthy children and rodents, as summarized in Wu et al. (2006). Therefore, signaling through a histamine receptor cascade may not be excluded. But usually $Zn^{2+}$ would rather potentiate but not reduce such carnosine- or histamine-mediated effects (O'Dowd and Miller 1998).

Another simple explanation could be that the opposite effect of $ZnCl_2$ in our study may arise from a poor solubility of $Zn^{2+}$ in artificial cerebrospinal fluids, which contain inorganic phosphate ($P_i$) (Rumschik et al. 2009).

Another more critical explanation may arise from the observations in the literature that the shortly applied anesthetic isoflurane also modulates by itself the excitability in the brain via GABA-dependent and GABA-independent mechanisms (Ying et al. 2009). In several brain regions, pharmacoresistant R-type voltage-gated $Ca^{2+}$ channels trigger inhibitory synaptic transmission as, for example, in the reticular thalamic nucleus in brain slices (Joksovic et al. 2009). Both membrane protein complexes are modulated by zinc ions. However, as we have administered isoflurane only very briefly (for less than 5 min), we tend to exclude a dominant interaction of isoflurane with histidine, which could in principle also explain the beneficial histidine effect.

## Conclusion

Our findings show that the CNS administration of trace metal divalent cations in mice is possible by circumventing the blood–brain barrier. Epidural fixation of plastic cannula and EEG electrodes allow for high-quality EcoG recordings. To our surprise, histidine, the buffer for divalent metal cations, contributes by itself also in a beneficial way to the intensity of kainate-induced seizures in the mouse brain, suggesting that endogenous divalent metal cations may be chelated or that zinc-sensitive transporters ion channels or neurotransmitter receptors are modulated, which has to be analyzed more in detail.

**Acknowledgements** We would like to especially thank Mrs. Renate Clemens for her dedication and hard work in this project.

**Funding** This study was funded by a DFG/German Research Foundation Grant (Schn 387/21-1 and /21-2).

## Compliance with ethical standards

**Conflict of interest** Part of this study was presented at Annual Meeting of the German and Austrian Society for Epileptology and the Swiss Epilepsy-Liga in Wien, May 3rd–6th, 2017. Dr. Maxine Dibué-Adjei is an Employee of LivaNova PLC. None of the authors has anything other to disclose. We confirm that we have read the Journal's position on issues involved in ethical publication and affirm that this report is consistent with those guidelines.

## References

Arakawa T (1974) Congenital and acquired disturbances of histidine metabolism. Clin Endocrinol Metab 3:17–35

Atkinson AJ (2017) Intracerebroventricular drug administration. Transl Clin Pharmacol 25:117–124

Blakemore LJ, Trombley PQ (2017) Zinc as a neuromodulator in the central nervous system with a focus on the olfactory bulb. Front Cell Neurosci 11:297

Büsselberg D, Platt B, Michael D, Carpenter DO, Haas HL (1994) Mammalian voltage-activated calcium channel currents are XX blocked by $Pb^{2+}$, $Zn^{2+}$, and $Al^{3+}$. J Neurophysiol 71:1491–1497

Catterall WA (2011) Voltage-gated calcium channels. Cold Spring Harb Perspect Biol 3:a003947

Cook AM, Mieure KD, Owen RD, Pesaturo AB, Hatton J (2009) Intracerebroventricular administration of drugs. Pharmacotherapy 29:832–845

Dibue-Adjei M, Kamp MA, Alpdogan S, Tevoufouet EE, Neiss WF, Hescheler J, Schneider T (2017) Cav2.3 (R-type) calcium channels are critical for mediating anticonvulsive and neuroprotective properties of lamotrigine in vivo. Cell Physiol Biochem 44:935–947

Edholm OG (1942) The effect of histidine on histamine shock. J Physiol 101:252–256

Fong CW (2015) Permeability of the blood–brain barrier: molecular mechanism of transport of drugs and physiologically important compounds. J Membr Biol 248:651–669

Frederickson CJ, Koh JY, Bush AI (2005) The neurobiology of zinc in health and disease. Nat Rev Neurosci 6:449–462

Honda T (1984) Amino acid metabolism in the brain with convulsive disorders. Part 2: The effects of anticonvulsants on convulsions and free amino acid patterns in the brain of El mouse. Brain Dev 6:22–26

Huang H, Li Y, Liang J, Finkelman FD (2018) Molecular regulation of histamine synthesis. Front Immunol 9:1392

Joksovic PM, Weiergraber M, Lee W, Struck H, Schneider T, Todorovic SM (2009) Isoflurane-sensitive presynaptic R-type calcium channels contribute to inhibitory synaptic transmission in the rat thalamus. J Neurosci 29:1434–1445

Kaminski RM, Zolkowska D, Kozicka M, Kleinrok Z, Czuczwar SJ (2004) L-Histidine is a beneficial adjuvant for antiepileptic drugs against maximal electroshock-induced seizures in mice. Amino Acids 26:85–89

Kang HW, Park JY, Jeong SW, Kim JA, Moon HJ, Perez-Reyes E, Lee JH (2006) A molecular determinant of nickel inhibition in Cav3.2 T-type calcium channels. J Biol Chem 281:4823–4830

Kang HW, Moon HJ, Joo SH, Lee JH (2007) Histidine residues in the IS3–IS4 loop are critical for nickel-sensitive inhibition of the Cav2.3 calcium channel. FEBS Lett 581:5774–5780

Kiss T, Osipenko O (1994) Metal ion-induced permeability changes in cell membranes: a minireview. Cell Mol Neurobiol 14:781–789

Lee JH, Gomora JC, Cribbs LL, Perez-Reyes E (1999) Nickel block of three cloned T-type calcium channels: low concentrations selectively block α1H. Biophys J 77:3034–3042

Li Q, Jin CL, Xu LS, Zhu-Ge ZB, Yang LX, Liu LY, Chen Z (2005) Histidine enhances carbamazepine action against seizures and improves spatial memory deficits induced by chronic transauricular kindling in rats. Acta Pharmacol Sin 26:1297–1302

Mathie A, Sutton GL, Clarke CE, Veale EL (2006) Zinc and copper: pharmacological probes and endogenous modulators of neuronal excitability. Pharmacol Ther 111:567–583

Neumaier F, Dibué-Adjei M, Hescheler J, Schneider T (2015) Voltage-gated calcium channels: determinants of channel function and modulation by inorganic cations. Prog Neurobiol 129:1–36

O'Dowd A, Miller DJ (1998) Analysis of an H1 receptor-mediated, zinc-potentiated vasoconstrictor action of the histidyl dipeptide carnosine in rabbit saphenous vein. Br J Pharmacol 125:1272–1280

Perez-Reyes E, Schneider T (1994) Calcium channels: structure, function, and classification. Drug Dev Res 33:295–318

Rumschik SM, Nydegger I, Zhao J, Kay AR (2009) The interplay between inorganic phosphate and amino acids determines zinc solubility in brain slices. J Neurochem 108:1300–1308

Shcheglovitov A, Vitko I, Lazarenko RM, Orestes P, Todorovic SM, Perez-Reyes E (2012) Molecular and biophysical basis of glutamate and trace metal modulation of voltage-gated Ca(v)2.3 calcium channels. J Gen Physiol 139:219–234

Takeda A, Suzuki M, Okada S, Oku N (2000) 65Zn localization in rat brain after intracerebroventricular injection of 65Zn-histidine. Brain Res 863:241–244

Valko M, Morris H, Cronin MT (2005) Metals, toxicity and oxidative stress. Curr Med Chem 12:1161–1208

Wadman SK, van Sprang FJ, van Stekelenburg GJ, de Bree PK (1966) Three new cases of Histidinemia. Clinical and biochemical data. Z Gesamte Inn Med 21:485–492

Weiergräber M, Henry M, Hescheler J, Smyth N, Schneider T (2005) Electrocorticographic and deep intracerebral EEG recording in mice using a telemetry system. Brain Res Brain Res Protoc 14:154–164

Wu XH, Ding MP, Zhu-Ge ZB, Zhu YY, Jin CL, Chen Z (2006) Carnosine, a precursor of histidine, ameliorates pentylenetetrazole-induced kindled seizures in rat. Neurosci Lett 400:146–149

Ying SW, Werner DF, Homanics GE, Harrison NL, Goldstein PA (2009) Isoflurane modulates excitability in the mouse thalamus via GABA-dependent and GABA-independent mechanisms. Neuropharmacology 56:438–447

**Publisher's Note** Springer Nature remains neutral with regard to jurisdictional claims in published maps and institutional affiliations.